Do free-falling quantum cats land on their feet?

2015 J. Phys. A: Math. Theor. 48 295301

(http://iopscience.iop.org/1751-8121/48/29/295301)

IOP Publishing Journal of Physics A: Mathematical and Theoretical
J. Phys. A: Math. Theor. **48** (2015) 295301 (17pp) doi:10.1088/1751-8113/48/29/295301

Do free-falling quantum cats land on their feet?

C Chryssomalakos[1], H Hernández-Coronado[2,3] and E Serrano-Ensástiga[1]

[1] Instituto de Ciencias Nucleares, Universidad Nacional Autónoma de México, Apartado Postal 70-543, México D.F. 04510, México
[2] Departamento de Física, CINVESTAV, A.P. 14-740, México D.F. 07000, México

E-mail: chryss@nucleares.unam.mx, hhernandez@fis.cinvestav.mx and eduardo.serrano@correo.nucleares.unam.mx

Received 19 January 2015, revised 19 May 2015
Accepted for publication 11 June 2015
Published 3 July 2015

Abstract

We present a quantum description of the mechanism by which a free-falling cat manages to reorient itself and land on its feet, having all along zero angular momentum. Our approach is geometrical, making use of the fiber bundle structure of the cat configuration space. We show how the classical picture can be recovered, but also point out a purely quantum scenario, that ends up with a Schroedinger cat. Finally, we sketch possible applications to molecular, nuclear, and nano-systems.

Keywords: geometrical methods, n-body problem, cat problem

(Some figures may appear in colour only in the online journal)

1. Introduction

Free falling cats, relying on their *feline righting reflex*, manage to land on their feet, even if released upside-down, and with zero initial angular momentum—all they need is a minimal distance of about thirty centimeters to the ground, although claims of much shorter distances exist, including the five centimeters reported by Maxwell [1]. The phenomenon is puzzling, as it seems to violate conservation of angular momentum, but a careful analysis, first carried through by Kane and Scher [2], shows that cats don't rotate *despite* angular momentum conservation, but, rather, *because* of it.

The emergence of geometrical methods in the study of the *n*-body problem, pioneered by Guichardet [3], revived the interest in the falling cat problem, leading to subsequent

[3] Author to whom any correspondence should be addressed.

refinements and extensions [4], including the influential work of Shapere and Wilczek [5], that embedded the subject in mainstream, application-oriented physics. On the more formal front, the culmination came with the *Falling Cat Theorem*, by Montgomery [6], converting this problem to the prototype of a whole class of classical dynamical systems exhibiting anholonomy. The quantum version of this approach has shed a new, bright light on molecular dynamics (see, e.g. [7–10]) providing far deeper insights than those accessible to the traditional approaches.

Our aim in this paper is to provide a quantum description of the falling, rotating cat, using the above mentioned geometrical approach. Needless to say, our model is not realistic: we study a triangular, quasi-rigid cat. But the essence of the phenomenon is captured already by such a simple model, with additional touches of detail expected to emerge through a four-point-mass model, which would naturally reveal the true non-abelian nature of the problem—larger numbers of points would probably add little, at the fundamental level.

Three body systems have been studied before, both in the classical and the quantum case. Of the recent literature, we single out the treatment in [11], as the most relevant to our own, at the classical level, and that of [12], at the quantum level. A much wider body of work exists related to applications to molecular physics. In this case, the presence of an electron cloud around the nuclei, and its adiabatic treatment in the Born–Oppenheimer scheme, gives rise to another gauge structure, distinct from the one mentioned above, which manifests itself in subtle phase effects—see for example [13, 14] and especially [15] for a review.

The structure of the paper is as follows: section 2 briefly reviews the classical and, then, quantum geometric description of the n-body problem, specifying the general results to the case of a quasi-rigid body, modelled like point masses connected by stiff elastic rods—here we follow closely [8]. The main part of the paper is in section 3, where the triangular model is presented and studied in detail. Potential implications for molecular, nuclear, and nano-systems are briefly sketched in section 4. Some concluding remarks appear in the last section.

2. Geometrical formulation of *n*-body dynamics

2.1. The classical description

We consider an isolated deformable body, modelled by n point-like particles, interacting among themselves through a potential V. The configuration space of the body is $C_{\text{tot}} = \mathbb{R}^{3n}$ and its Lagrangian is given by

$$L_{\text{tot}} = \frac{1}{2}\sum_{\alpha=1}^{n} m_\alpha \left|\dot{\mathbf{r}}_{s\alpha}\right|^2 - V(\mathbf{r}_{s,1}, \ldots, \mathbf{r}_{s,n}), \tag{1}$$

where $\mathbf{r}_{s\alpha} \in \mathbb{R}^3$ is the α-th particle's position vector with respect to a fixed (or space) frame (hence the s sub-index), and m_α its mass ($\alpha = 1, 2, \ldots, n$), while overdots denote time derivatives. The absence of external forces suggests the elimination of the translational degrees of freedom by introducing relative coordinates, e.g., the mass-weighted Jacobi coordinates,

$$\boldsymbol{\rho}_{s\alpha} = \sqrt{\mu_\alpha}\sum_{\beta=1}^{n} T_{\alpha\beta}\mathbf{r}_{s\beta},\ \alpha = 1, \ldots, n-1, \tag{2}$$

where the μ_α are reduced masses and $T_{\alpha\beta}$ is a suitable numerical matrix (see [8] for the details).

Under the coordinate transformation (2), the kinetic energy of the center of mass separates from the total kinetic energy, and thus the Lagrangian can be written as $L_{\text{tot}} = L_{\text{CM}} + L$,

with

$$L_{\mathrm{CM}} = \frac{1}{2} M \left|\dot{\mathbf{R}}_s\right|^2, \qquad L = \frac{1}{2}\sum_{\alpha=1}^{n-1}\left|\dot{\boldsymbol{\rho}}_{s\alpha}\right|^2 - V\left(\boldsymbol{\rho}_{s,1}, \ldots, \boldsymbol{\rho}_{s,n-1}\right), \tag{3}$$

where $M = \sum_{\alpha=1}^{n} m_\alpha$ and $\mathbf{R}_s = M^{-1}\sum_{\alpha=1}^{n} m_\alpha \mathbf{r}_{s\alpha}$.

Likewise, in these coordinates it is clear that the total configuration space can be written as $\mathcal{C}_{\mathrm{tot}} = \mathbb{R}^3 \times \mathcal{C}$, where $\mathcal{C} = \mathbb{R}^{3n-3}$ is the translation-reduced configuration space, on which $(\boldsymbol{\rho}_{s,1}, \ldots, \boldsymbol{\rho}_{s,n-1})$ are coordinates. For the rest of the paper we assume that $\mathbf{R}_s = 0$ and refer to $\mathcal{C}$ simply as *the* configuration space. A point in $\mathcal{C}$ is specified once the body's shape and orientation are given. There are $3n-6$ coordinates q^μ needed to specify the body's shape, which correspond to independent functions on configuration space, invariant under proper rotations, i.e.,

$$q^\mu\left(\boldsymbol{\rho}_{s,1}, \ldots, \boldsymbol{\rho}_{s,n-1}\right) = q^\mu\left(\mathsf{Q}\boldsymbol{\rho}_{s,1}, \ldots, \mathsf{Q}\boldsymbol{\rho}_{s,n-1}\right), \quad \text{for all } \mathsf{Q} \in SO(3). \tag{4}$$

Defining the body's orientation, on the other hand, requires (i) an orthonormal frame, fixed to the body for each shape, given by relations[4] $\boldsymbol{\rho}_\alpha = \boldsymbol{\rho}_\alpha(q^\mu)$, $\alpha = 1, \ldots, n-1$, and (ii) the rotation $\mathsf{R} \in SO(3)$ that maps the above body frame to the fixed space frame, parametrized, for example, by Euler angles, $\mathsf{R} = \mathsf{R}(\theta^i)$. Fixing a body frame for each shape is a choice of gauge, that defines as reference orientation the one where the body and the space frames coincide. The factorization of (non-collinear) configurations in 'shape times orientation' leads to a description of $\mathcal{C}$ as a $SO(3)$ principal fibre bundle, with base the 'shape space' $\mathcal{S} = \mathbb{R}^{3n-3}/SO(3)$ and fibre diffeomorphic to $SO(3)$. Another fact worth mentioning is that the above fibre bundle is in general non-trivial, so that a section cannot be chosen globally, in other words, there is no smooth assignment of a body frame to all shapes.

In terms of these orientation and shape coordinates, (θ^i, q^μ), and a section $\boldsymbol{\rho}_\alpha(q^\mu)$ as above, a point $(\boldsymbol{\rho}_{s,1}, \ldots, \boldsymbol{\rho}_{s,n-1})$ in $\mathcal{C}$ is defined by

$$\boldsymbol{\rho}_{s,\alpha} = \mathsf{R}\left(\theta^i\right)\boldsymbol{\rho}_\alpha\left(q^\mu\right), \ \alpha = 1, \ldots, n-1. \tag{5}$$

The above relation expresses the fact that given a shape of the body q^μ, and a reference orientation $\boldsymbol{\rho}_\alpha(q^\mu)$, any configuration of the body, with that shape, can be reached through a unique rotation $\mathsf{R}(\theta^i)$. For the tangent space $T\mathcal{C}$, it will prove convenient to use an anholonomic basis, such that the velocity vector $\mathbf{v}$ of the system has components $v^a = (\boldsymbol{\omega}^i, \dot{q}^\mu)$, where

$$\omega^i = -\frac{1}{2}\epsilon^{ijk}\left(\mathsf{R}^{\mathsf{T}} \cdot \dot{\mathsf{R}}\right)_{jk} \tag{6}$$

is the i-th component of the angular velocity of the body frame w.r.t. the space frame, referred to the body frame (as indicated by the absence of subscript s)—the corresponding basis vectors satisfy the $\mathfrak{so}(3)$ Lie algebra. In the above expression, and in what follows, we employ the Einstein summation convention for repeated indices.

We may now recast the Lagrangian (3) in the form

$$L = \frac{1}{2} G_{ab} v^a v^b - V(q), \qquad \left(G_{ab}\right) \equiv \begin{pmatrix} \mathsf{M} & \mathsf{M}\cdot\mathbf{A}_\nu \\ A_\mu \cdot \mathsf{M} & g_{\mu\nu} + \mathbf{A}_\mu \cdot \mathsf{M} \cdot \mathbf{A}_\nu \end{pmatrix}, \tag{7}$$

[4] The absence of the sub-index s in a vector, will henceforth imply that its components are referred to the body frame.

where (G_{ab}) is the metric in configuration space $\mathcal{C}$, defined by the kinetic energy, M is the inertia tensor, and

$$\mathbf{A}_\mu = \mathsf{M}^{-1} \cdot \sum_{\alpha=1}^{n-1} \boldsymbol{\rho}_\alpha \times \frac{\partial \boldsymbol{\rho}_\alpha}{\partial q^\mu}, \qquad g_{\mu\nu} = \sum_{\alpha=1}^{n-1} \frac{\partial \boldsymbol{\rho}_\alpha}{\partial q^\mu} \cdot \frac{\partial \boldsymbol{\rho}_\alpha}{\partial q^\nu} - \mathbf{A}_\mu \cdot \mathsf{M} \cdot \mathbf{A}_\nu, \tag{8}$$

are the Coriolis gauge potential and the metric on shape space $\mathcal{S}$, respectively.

A velocity vector of the form $v^a = (\boldsymbol{\omega}, 0)$ is purely rotational, or *vertical*, since $\dot{q}^\mu = 0$ implies the body's shape is not changing. A complementary notion of horizontality is furnished by decreeing a velocity vector *horizontal* if the corresponding motion of the system has zero total angular momentum. It turns out that horizontal and vertical vectors are orthogonal according to the above metric G. In the anholonomic basis introduced earlier, the angular momentum, referred to the body frame, is given by

$$\mathbf{L} = \mathsf{M} \cdot \left(\boldsymbol{\omega} + \mathbf{A}_\mu \dot{q}^\mu\right), \tag{9}$$

and thus, vanishing angular momentum implies $\boldsymbol{\omega} \mathrm{d}t = -\mathbf{A}_\mu \mathrm{d}q^\mu$. In this case, $\mathbf{A}_\mu$ maps infinitesimal changes in shape space to infinitesimal rotations, so that the horizontal lift in $\mathcal{C}$ of a given path $q^\mu(t)$ in shape space has orientational coordinates given by

$$\mathsf{R}(t) = \mathcal{P} \exp\left(-\int_{q_0}^{q(t)} \mathsf{A}_\mu \mathrm{d}q^\mu\right), \tag{10}$$

where the space and body frames were assumed in coincidence at $t = 0$, $\mathcal{P}$ exp is the path-ordered exponential, and the antisymmetric matrix A_μ is related to the gauge potential via $(\mathsf{A}_\mu)_{ij} = -\epsilon_{ijk} A_\mu^{\ k}$.

Just as in Yang–Mills gauge field theory, it is possible to define an associated curvature 2-form $\mathbf{B}$, called, in this case, the *Coriolis* tensor, with components given by

$$\mathbf{B}_{\mu\nu} = \partial_\mu \mathbf{A}_\nu - \partial_\nu \mathbf{A}_\mu - \mathbf{A}_\mu \times \mathbf{A}_\nu, \tag{11}$$

such that a cyclic deformation in shape space, with $\mathbf{L} = 0$, around the infinitesimal parallelogram spanned by the vectors y^μ and z^μ, produces the gauge-covariant infinitesimal rotation generated by $\boldsymbol{\omega} \mathrm{d}t = -\mathbf{B}_{\mu\nu} y^\mu z^\nu$. Note that $\mathsf{R} \neq \mathsf{I}$ requires both $\mathbf{B} \neq 0$ and a non-zero enclosed area by the closed path $q^\mu(t)$ in shape space.

The dynamics of the system can also be described by means of the gauge-covariant Hamiltonian

$$H = \frac{1}{2} \mathbf{L} \cdot \mathsf{M} \cdot \mathbf{L} + \frac{1}{2}\left(p_\mu - \mathbf{A}_\mu \cdot \mathbf{L}\right) g^{\mu\nu} \left(p_\nu - \mathbf{A}_\nu \cdot \mathbf{L}\right) + V(q), \tag{12}$$

where $p_\mu = g_{\mu\nu} \dot{q}^\nu + \mathbf{A}_\mu \cdot \mathbf{L}$ is the momentum conjugate to the shape coordinate q^μ. For $\mathbf{L} = 0$, (12) shows that the shape and orientation degrees of freedom decouple and one can solve independently for $q^\mu(t)$, plug it into expression (10), and obtain the orientation trajectory in $SO(3)$. Note that by assuming the system to be isolated, its shape evolution is entirely due to its own internal dynamics, rather than the action of external agents—this is consistent with what happens with a falling cat.

2.2. The quantum description

Up to this point, our analysis has been classical, although the particular ordering chosen in (12) makes it valid in the quantum case as well[5]. In this latter case, the body will be, in general, in a superposition of states, each corresponding to a definite shape and orientation—the general quantum state then will be described by a wavefunction $\Psi(\mathsf{R}, q)$ on $\mathcal{C}$ which, for the quasi-classical states that interest us, will be mostly concentrated around some mean shape and orientation. The closed circuit $q^\mu(t)$ in shape space, considered in the classical case, will be replaced, in the quantum case, by a similar circuit of the expectation value $\langle\Psi|q^\mu|\Psi\rangle$, while the resulting classical rotation at the end of the cycle will correspond to a vertical shift in the support of Ψ. Similarly, the classical condition $\mathbf{L} = 0$ will have to be replaced by the vanishing of the expectation value of each of the components of $\mathbf{L}$, as the restriction to zero angular momentum states is incompatible with the localization properties of Ψ in $\mathcal{C}$ mentioned above.

The hamiltonian H given in (12) commutes with $\mathbf{L}^2$ and L_{sz}, so its eigenfunctions can be chosen to be simultaneous eigenfunctions of all three operators, with eigenvalues, say, E, l, m, respectively, which we denote by $\psi_{lm}(\mathsf{R}, q)$, suppressing the index E. Standard properties of these functions (see, e.g., [16], section 58) imply that

$$\psi_{lm}(\mathsf{R}, q) = \sum_{k=-l}^{l} \chi_k^l(q) D_{mk}^l(\mathsf{R})^*, \tag{13}$$

where $D_{km}^l(\mathsf{R})$ are the Wigner functions corresponding to the $(2\,l + 1) \times (2\,l + 1)$ irreducible matrix representation of $\mathsf{R} \in SO(3)$, and $\chi_k^l(q)$ is (proportional to) the value of ψ_{lm} on the section Σ,

$$\chi_k^l(q) = \frac{1}{\sqrt{2\,l + 1}} \psi_{lk}(\mathsf{I}, q). \tag{14}$$

In this way, the orientational part of the problem has been taken care of by group theory—substituting the above ψ_{lm} in (12), H becomes a $2l$+1-dimensional matrix, with entries depending on the operators q^μ, p_ν, acting on the column vector (χ_k^l), whose components, indexed by k, depend on q. The resulting eigenvalue equation which, with a slight abuse of notation, we write as $H\chi_k^l = E\chi_k^l$, is still a formidable problem to solve, as M, $\mathbf{A}_\mu$, $g_{\mu\nu}$, V, are all, in general, complicated functions of the q's. For our purposes though, it is enough to observe the cat's rotation for small deformations of its shape, so we adopt, in what follows, a perturbative approach.

2.3. The quasi-rigid approximation

We imagine now that the interaction potential V is due to elastic, but stiff, rods, that connect the n point masses. At their equilibrium length, the rods give the body the shape q_0, which we assume non-collinear, while when slightly deformed, the body's shape is $q^\mu = q_0^\mu + \lambda x^\mu$, where λ is a small dimensionless parameter. Expanding the potential V around q_0, we obtain a system of coupled harmonic oscillators, small vibrations of which will provide the cyclic shape change we seek. So far the $\mathcal{S}$-coordinates q have been taken arbitrary, but we now have enough motivation to choose them in a very special way: first, the directions $\partial_\mu \equiv \partial/\partial q^\mu$ will be taken to be those of the normal modes of the system, so that the expansion of V around q_0

[5] The complete expression for the quantum operator H involves a new potential term $V_2(q)$ [8], which we ignore here as it will be irrelevant in the particular applications we consider.

is diagonalized,

$$V(q) = \frac{1}{2}\sum_{\mu=1}^{3n-6}\frac{\omega_{(\mu)}^2}{\lambda^2}x_\mu x^\mu, \tag{15}$$

where we have assumed that $V(q_0) = 0$ and that $\partial_\mu^2 V = \omega_{(\mu)}^2/\lambda^4$. This latter assumption simply means that we chose the scale of the masses of the particles so that the resulting oscillation frequencies are of order λ^{-2}. Having fixed the directions ∂_μ, we now extend the q-lines (or, what is the same, the x-lines) so that they be geodesics of the $\mathcal{S}$-metric $g_{\mu\nu}$, obtaining Riemann normal coordinates on $\mathcal{S}$. This latter property of the coordinates guarantees that no linear terms appear in the expansion of the metric around q_0,

$$g_{\mu\nu}(x) = \delta_{\mu\nu} + \frac{1}{3}\lambda^2 R_{\mu\alpha\beta\nu}(0)x^\alpha x^\beta + O\left(\lambda^3\right), \tag{16}$$

where the zeroth order term was made equal to the unit matrix by suitable normalization of the q's. Expression (16) implies that the corresponding Christoffel symbols satisfy $\Gamma^\alpha_{\mu\nu}x^\mu x^\nu = 0$.

There is one final simplifying choice we can make, and that is of the gauge potential $\mathbf{A}_\mu$. We opt for the Poincaré (or, transversal) gauge, centered at q_0, so that

$$\mathbf{A}_\mu(x) = \frac{\lambda}{2}\mathbf{B}_{\mu\alpha}(0)x^\alpha + O\left(\lambda^2\right), \tag{17}$$

which, on the one hand, makes $\mathbf{A}_\mu(0)$ equal to zero, and, on the otherhand, expresses H in terms of the gauge-covariant tensor $\mathbf{B}$. The above expression for $\mathbf{A}$ in terms of $\mathbf{B}$ can be obtained by applying the Poincaré homotopy operator, appropriately generalized to the non-abelian case [17]. In geometrical terms, the corresponding section Σ is the horizontal lift of radial lines, in the coordinates used, emerging from the equilibrium configuration. When the coordinates are Riemann normal coordinates, as above, the section is flat, and the corresponding choice of body frame is that of Eckart [18].

Finally, we rescale various quantities according to

$$p_\mu \to p_\mu/\lambda, \quad H \to \lambda^2 H, \quad \mathsf{M} \to \lambda^2\mathsf{M}, \quad \mathbf{A}_\mu \to \lambda\mathbf{A}_\mu, \quad \mathbf{L} \to \mathbf{L}, \tag{18}$$

and express $R_{\mu\alpha\beta\nu}$ in terms of $\mathbf{B}_{\mu\nu}$,

$$2R_{\mu\nu\sigma\tau} = \mathbf{B}_{\mu\nu}\cdot\mathsf{M}\cdot\mathbf{B}_{\sigma\tau} + \mathbf{B}_{\mu[\tau}\cdot\mathsf{M}\cdot\mathbf{B}_{\sigma]\nu}, \tag{19}$$

(see relation (5.61) from [8]), so that H can be expanded as

$$H = \frac{1}{2}\left(\sum_{\mu=1}^{3n-6}p^\mu p_\mu + \omega_{(\mu)}^2 x^\mu x_\mu\right) + \frac{1}{2}\lambda^2(\mathbf{L}-\mathbf{S})\cdot\mathsf{M}^{-1}\cdot(\mathbf{L}-\mathbf{S}). \tag{20}$$

The metric $g_{\mu\nu}$ implicit in the above expression, as well as M^{-1}, are both evaluated at q_0, and we have introduced the 'internal angular momentum' $\mathbf{S}$, and the 'shape angular momentum' S,

$$\mathbf{S} = \frac{1}{4}\mathsf{M}\cdot\mathbf{B}_{\mu\nu}S^{\mu\nu}, \quad S^{\mu\nu} = x^\mu p^\nu - x^\nu p^\mu, \tag{21}$$

with $\mathbf{B}_{\mu\nu}$ also evaluated at q_0. The shape and orientation degrees of freedom are only coupled by the cross terms, proportional to $\mathbf{L}\cdot\mathsf{M}^{-1}\cdot\mathbf{S}$ and $\mathbf{S}\cdot\mathsf{M}^{-1}\cdot\mathbf{L}$ in (20), which can be interpreted as infinitesimal rotations about the unit vector $\widehat{\mathsf{M}^{-1}\cdot\mathbf{S}}$ by an angle $|\mathsf{M}^{-1}\cdot\mathbf{S}|$, both

of the latter quantities being operators in shape space. Te see this explicitly, we consider the simplest non-trivial case, the three point cat.

3. A minimal cat: the three-body model

3.1. Three-body dynamics

As it turns out, to 'see' the cat rotating while it changes its shape, it is enough to model it as a three-point-mass system. In this case the shape space has dimension $3n - 6 = 3$ and we can define $n - 1 = 2$ Jacobi vectors as

$$\boldsymbol{\rho}_{s1} = \sqrt{\mu_1}\,(\mathbf{r}_{s1} - \mathbf{r}_{s3}), \qquad \boldsymbol{\rho}_{s2} = \sqrt{\mu_2}\left(\mathbf{r}_{s2} - \mathbf{R}_{s,13}\right), \tag{22}$$

where

$$\mu_1 = \frac{m_1 m_3}{m_1 + m_3}, \quad \mu_2 = \frac{m_2(m_1 + m_3)}{m_1 + m_2 + m_3}, \quad \mathbf{R}_{s,13} = \frac{m_1\mathbf{r}_{s1} + m_3\mathbf{r}_{s3}}{m_1 + m_3}. \tag{23}$$

A convenient set of coordinates in shape space is (we switch to lower indices for typographical convenience)[6]

$$q_1 = \left|\boldsymbol{\rho}_{s1}\right|^2 - \left|\boldsymbol{\rho}_{s2}\right|^2, \qquad q_2 = 2\boldsymbol{\rho}_{s1}\cdot\boldsymbol{\rho}_{s2}, \qquad q_3 = 2\left|\boldsymbol{\rho}_{s1}\times\boldsymbol{\rho}_{s2}\right| \geqslant 0, \tag{24}$$

mapping $\mathcal{S}$ to the upper half of $\mathbb{R}^3$. The q_3 coordinate measures the area of the (triangular) body, so that the plane $q_3 = 0$ corresponds to collinear shapes, while the q_3 axis to symmetric ones, i.e., those whose inertia tensor is degenerate in the body $x - y$ plane. In the principal-axis gauge, $\mathbf{A}$ is given by

$$\mathbf{A}_\mu \mathrm{d}q^\mu = \frac{q_1\mathrm{d}q_2 - q_2\mathrm{d}q_1}{2q\left(q_1^2 + q_2^2\right)}\,\hat{\mathbf{z}}, \tag{25}$$

where $q^2 = q_1^2 + q_2^2 + q_3^2$, while $\mathbf{B}_{\mu\nu}$ turns out to be

$$\mathbf{B}_{\mu\nu} = \frac{1}{2q^3}\epsilon_{\mu\nu\alpha}q^\alpha\,\hat{\mathbf{z}}. \tag{26}$$

The last two expressions show that $\mathbf{A}$ has a string singularity along the q_3-axis, while $\mathbf{B}$ resembles a magnetic monopole, located at the origin of $\mathcal{S}$. The string singularity of $\mathbf{A}$ is related to the fact that, on the q_3-axis, the principal axis frame is itself singular, that is, the functions $\boldsymbol{\rho}_\alpha(q^\mu)$, that define the body frame, are not differentiable there [9]. In fact, it is easy to show that in going around the q_3-axis once in a circle the principal axes in the plane of the triangle reverse their direction, and this holds true regardless of the radius of the circle, a classical fact that is echoed in the sign change of the wavefunction in going around 'diabolical points' in the spectrum of multiparametric hamiltonians (see, e.g., [13, 19]). This singularity is relevant because the section wavefunction $\chi_k^l(q^\mu)$ is itself singular at the same places the gauge potential is, but can be relocated by changing the gauge (it cannot be eliminated though). For instance, by going to the so-called 'north-regular gauge', which is obtained from the principal-axis one by a rotation around the body z-axis by an angle of $-\arctan(q_2/q_1)/2$, the singularity can be relocated to the negative q_3-axis, which is not part of $\mathcal{S}$ [8]. On the other hand, the singularity of $\mathbf{B}$ is immune to gauge transformations.

[6] Radically different coordinates in the space of triangles can be and have been used—see, e.g., [19].

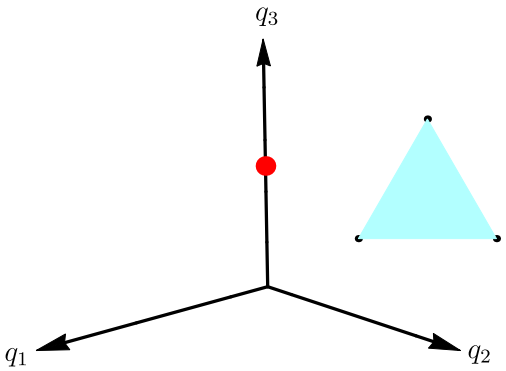

Figure 1. The three-body equilibrium point q_0 is represented in abstract shape space by the dot on the q_3-axis. The corresponding shape is an equilateral triangle of unit side, also illustrated in the figure.

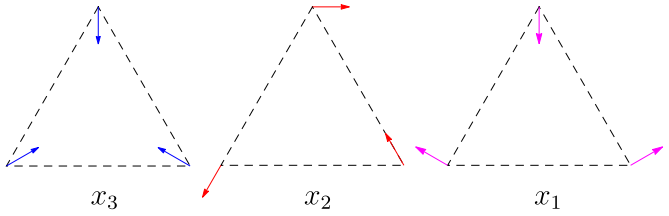

Figure 2. The normal modes of oscillation of the three body system when the equilibrium shape corresponds to an equilateral triangle. From left to right, the breather (or *symmetric stretching*) mode x_3, the *bending* mode x_2, and the *asymmetric stretching* mode x_1, the latter two being degenerate in frequency.

3.2. Quasi-rigid triangular cat

The singular behaviour of the wavefunction can be avoided in this case by adopting the north regular gauge, which is also an Eckart, and Poincaré gauge, centered on the equilibrium point $q_0 = (q_0^1, q_0^2, q_0^3) = (0, 0, 1)$. The latter corresponds to an equilateral triangle shape, of unit distance between the masses, as shown in figure 1. We make a linear coordinate transformation,

$$\tilde{q}_1 = -\frac{1}{3}q_1 + \frac{\sqrt{2}}{3}q_2, \quad \tilde{q}_2 = -\frac{\sqrt{2}}{3}q_1 - \frac{1}{3}q_2, \quad \tilde{q}_3 = -\frac{1}{2}q_3, \tag{27}$$

so that $\tilde{q}_0 = (0, 0, -1/2)$, and the x's, defined in the standard way by $\tilde{q}^\mu = \tilde{q}_0^\mu + \lambda x^\mu$, are normal modes. x_3 corresponds to the (highest frequency) breathing mode with $\omega_3 = \sqrt{2}$ (in natural units), while x_1 and x_2 are degenerate orthogonal modes of frequency $\omega_1 = \omega_2 = 1$, the corresponding patterns of oscillation are illustrated in figure 2.

The moment of inertia tensor for the equilibrium shape is

$$\mathsf{M} = \begin{pmatrix} 1/2 & 0 & 0 \\ 0 & 1/2 & 0 \\ 0 & 0 & 1 \end{pmatrix}, \tag{28}$$

while the only non-trivial component of the Coriolis tensor is $\mathbf{B}_{12} = 2\hat{\mathbf{z}}$ and therefore the 'internal angular momentum' reduces to $\mathbf{S} = S_{12}\hat{\mathbf{z}}$, where $S_{12} = x_1 p_2 - x_2 p_1$ is the shape

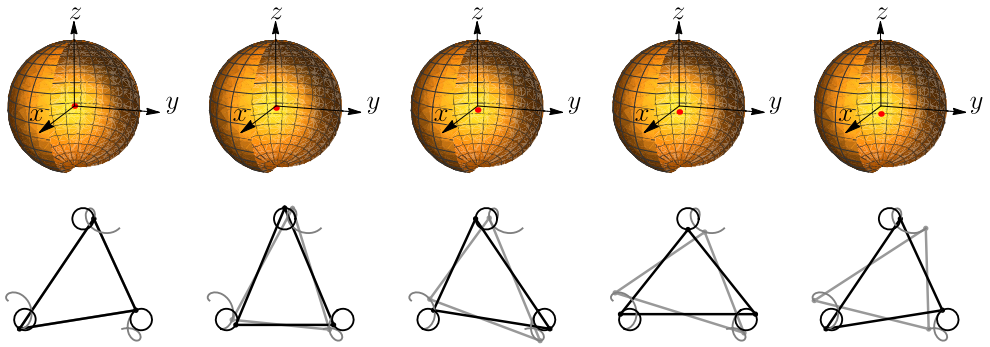

Figure 3. Sequence of the orientation change produced by a cyclic deformation in the x_1–x_2 plane in shape space, for the three body problem. The ball on the top row is $SO(3)$ in the axis-angle representation. Snapshots at times $t = 2\pi n/4$ are shown, with $n = 0, 1, \ldots, 4$, for $S_{12} = 4$ and $\lambda = 0.2$. The little dot close to the origin of $SO(3)$ represents the orientation of the body frame, with the corresponding shape shown just below, both in the body (black) and lab (grey) frame. For purposes of illustration, the deformation w.r.t. the equilibrium equilateral configuration, has been visually exaggerated by a factor of 4. The downwards motion of the dot signals a clockwise rotation of the body frame around the z-axis. The little black circles on the vertices of the triangle are the trajectories of these vertices in the body frame. The grey cycloid-like curves are the same trajectories in the lab frame.

angular momentum in the x_1–x_2 plane. Accordingly, the hamitonian takes the form

$$H = \frac{1}{2}\left(p_1^2 + p_2^2 + x_1^2 + x_2^2\right) + \frac{1}{2}\left(p_3^2 + 2x_3^2\right) + \lambda^2\left(\mathbf{L}^2 - \frac{1}{2}L_z^2 - L_z S_{12} + \frac{1}{2}S_{12}^2\right). \tag{29}$$

3.2.1. The classical case. As mentioned before, in the classical case the condition of vanishing angular momentum makes it possible to find the solutions of the equations of motion for the shape coordinates independently of the orientation ones. For the above hamiltonian, S_{12} is a constant of the motion, with $x^\mu(t)$ being harmonic oscillators, to leading order in λ,

$$x^\mu(t) = x_0^\mu \cos\omega_\mu t + \frac{p_0^\mu}{\omega_\mu}\sin\omega_\mu t, \tag{30}$$

with frequencies $\omega_\mu = (1, 1, \sqrt{2})$ and $p^\mu(t) = \dot{x}^\mu(t)$. Equation (10) then gives

$$\mathsf{R}(t) = \begin{pmatrix} \cos\left(\lambda^2 S_{12} t\right) & \sin\left(\lambda^2 S_{12} t\right) & 0 \\ -\sin\left(\lambda^2 S_{12} t\right) & \cos\left(\lambda^2 S_{12} t\right) & 0 \\ 0 & 0 & 1 \end{pmatrix}, \tag{31}$$

which represents a rotation about $\hat{\mathbf{z}}$ by an angle $\alpha(t) = -\lambda^2 S_{12} t$, so that the cyclic shape change (30) with $x_3(t) = 0 = p_3(t)$ gives rise to $\alpha(2\pi) = -2\pi\lambda^2 S_{12}$. In figure 3 we show the cyclic deformation sequence that produces the rotation (31), for $S_{12} = 4$, and a total time interval of one period, $0 \leqslant t \leqslant T = 2\pi/\omega_1$. Note that the triangle is deformed, w.r.t. the equilateral configuration, at all times, since its trajectory in shape space is a circle *centered* on

(and, hence, never passing through) that configuration. Flipping the sign of S_{12} gives rise to a rotation in the opposite sense.

3.2.2. The quantum case. Turning now to the quantum case, we define the anihilation and creation operators for excitations along the three coordinate axes in shape space ($\hbar = 1$, $\mu = 1, 2, 3$),

$$a_\mu = \frac{1}{\sqrt{2}}\left(\sqrt{\omega_{(\mu)}}\, x_\mu + \frac{\mathrm{i}}{\sqrt{\omega_{(\mu)}}}\, p_\mu\right), \qquad a_\mu^\dagger = \frac{1}{\sqrt{2}}\left(\sqrt{\omega_{(\mu)}}\, x_\mu - \frac{\mathrm{i}}{\sqrt{\omega_{(\mu)}}}\, p_\mu\right), \tag{32}$$

as well as the circular analogues of the first two,

$$a_\pm = \frac{1}{\sqrt{2}}(a_1 \mp \mathrm{i}a_2), \qquad a_\pm^\dagger = \frac{1}{\sqrt{2}}\left(a_1^\dagger \pm \mathrm{i}a_2^\dagger\right), \tag{33}$$

and the associated number operators

$$N_\mu = a_\mu^\dagger a_\mu, \qquad N_\pm = a_\pm^\dagger a_\pm. \tag{34}$$

In terms of these, the hamiltonian (29) takes the form ($\omega_{1,2} = 1$)

$$H = (N + 1) + \omega_3\left(N_3 + \frac{1}{2}\right) + \lambda^2\left(\mathbf{L}^2 - \frac{L_z^2}{2} - SL_z + \frac{S^2}{2}\right), \tag{35}$$

with $N = N_+ + N_-$ and $S = N_+ - N_-$, acting on the Hilbert space $L^2(C, \mathrm{d}^3q\ \mathrm{dR})$, where dR is the normalized Haar measure in $SO(3)$. A complete set of mutually compatible operators, commuting with the hamiltonian, is $\{N, S, N_3, \mathbf{L}^2, L_{sz}, L_z\}$ (see [16]), so that hamiltonian eigenstates are labeled as $|n, s, n_3, l, m, k\rangle$, with $n_3, n, l \in \{0, 1, 2, \ldots\}$, $m, k = -l, -l+1, \ldots, l-1, l$ and $s = -n, -n+2, \ldots, n-2, n$. We are now ready to see the cat rotating, which we choose to do using Majorana's constellations.

3.3. Rotations in Majorana's stellar representation

Given an arbitrary spin-l state

$$|\psi\rangle = \sum_{k=-l}^{l} c_k\, |l, k\rangle, \tag{36}$$

Majorana's polynomial $p_{|\psi\rangle}(\zeta)$ can be associated to it,

$$p_{|\psi\rangle}(\zeta) = \sum_{k=-l}^{l} (-1)^{l-k}\sqrt{\binom{2\,l}{l-k}}\, c_k\, \zeta^{l+k}, \tag{37}$$

where ζ is a complex variable. The $2\,l$ roots of $p_{|\psi\rangle}$ can be mapped to $2\,l$ points (*stars*) on the 2-sphere via stereographic projection. The resulting *constellation*, consisting of the $2\,l$ stars, is the stellar representation of the state $|\psi\rangle$. If $c_k = 0$ for $k = l, l-1, \ldots, l-m$, then $\zeta = \infty$ is considered a root of multiplicity $m + 1$, resulting in the appearance of $m + 1$ stars at the north pole of S^2. The particular choice of coefficients in (37) results in that a rotation $D(\mathsf{R})$ of $|\psi\rangle$ in Hilbert space corresponds to a rotation R of the corresponding constellation on S^2 [20]. Thus, we will monitor any rotations of $|\psi\rangle$ by visual inspection of its constellation. We take as initial state of the system the following,

$$|\psi\rangle = \frac{1}{\sqrt{2}}\Big(\big|n,\, s,\, n_3,\, 1,\, 0,\, 1\big\rangle + \big|n,\, s,\, n_3,\, 1,\, 0,\, -1\big\rangle\Big) \equiv \big|n,\, s,\, n_3\big\rangle \otimes |\phi\rangle, \tag{38}$$

where $|\phi\rangle \equiv (|1,\, 0,\, 1\rangle + |1,\, 0,\, -1\rangle)/\sqrt{2}$ is the rotational state of the triangle, with Majorana polynomial[7]

$$p_{|\phi\rangle}(\zeta) = \frac{1}{\sqrt{2}}\Big(\zeta^2 + 1\Big), \tag{39}$$

the roots of which are $\zeta_\pm = \pm i$, and is therefore represented on S^2 by the pair of points $(x_\pm,\, y_\pm,\, z_\pm) = (0,\, \pm 1,\, 0)$ (see figure 4). It is easily seen that $\langle\phi|\mathbf{L}|\phi\rangle = 0$ holds, and that the only non-trivial time evolution of $|\psi(t)\rangle \equiv |n,\, s,\, n_3\rangle \otimes |\phi(t)\rangle$ comes from the term $-\lambda^2 L_z S$ in the hamiltonian, resulting in the Majorana polynomial for $|\phi(t)\rangle$

$$p_{|\phi(t)\rangle}(\zeta) \sim \zeta^2 + \mathrm{e}^{-2\mathrm{i}\lambda^2 st}, \tag{40}$$

the roots of which are $\zeta_\pm = \pm \mathrm{i}\mathrm{e}^{-\mathrm{i}\lambda^2\, st}$, with the corresponding stars at $(x_\pm,\, y_\pm,\, z_\pm) = \pm\Big(\sin(\lambda^2 st),\, \cos(\lambda^2\, st),\, 0\Big)$ (figure 4). Thus, the state $|\psi(t)\rangle$ rotates with time about $\hat{\mathbf{z}}$ by an angle $-\lambda^2\, st$, in complete agreement with what we found classically. Even so, the correspondence with the classical analysis is limited in this case, in that $|\psi(t)\rangle$ is not a state of well defined shape or orientation, nor is it obvious that the rotation found can be somehow associated with a cyclic change of the body's shape. We can do better, in this respect, by considering coherent states in shape space.

3.4. Coherent state falling cat

We consider now the state ($\alpha_\pm \in \mathbb{C}$)

$$\Psi(\mathsf{R},\, q) = \psi_{\alpha_+,\alpha_-}(x_1,\, x_2)\psi_0(x_3)\Phi(\phi), \tag{41}$$

where

$$\psi_{\alpha_+,\alpha_-}(x_1,\, x_2) = \frac{1}{\sqrt{\pi}}\prod_{i=1}^{2}\ \mathrm{e}^{-\frac{1}{2}\left(x_i - \langle x_i\rangle\right)^2}\mathrm{e}^{\mathrm{i}\left\langle p_i\right\rangle\left(x_i - \frac{1}{2}\langle x_i\rangle\right)}, \tag{42}$$

is a coherent state,

$$\begin{aligned}\psi_{\alpha_+,\alpha_-}(x_1,\, x_2) &= \big\langle x_1,\, x_2,\, \big|\ \alpha_+,\, \alpha_-\big\rangle \\ &= \Big\langle x_1,\, x_2\Big|\exp\Big(\alpha_+ a_+^\dagger - \alpha_+^* a_+\Big)\exp\Big(\alpha_- a_-^\dagger - \alpha_-^* a_-\Big)|0,\, 0\rangle,\end{aligned} \tag{43}$$

with

$$\left\langle x_i\right\rangle = \sqrt{2}\ \ \mathrm{Re}(\alpha_i), \quad \left\langle p_i\right\rangle = \sqrt{2}\ \ \mathrm{Im}(\alpha_i), \quad i\ =\ 1,\, 2, \tag{44}$$

$$\alpha_1 = \frac{1}{\sqrt{2}}(\alpha_+ + \alpha_-), \quad \alpha_2 = \frac{i}{\sqrt{2}}(\alpha_+ - \alpha_-), \tag{45}$$

$\psi_0(x_3)$ is the breathing mode ground state, and $\Phi(\phi) = \Phi(\mathsf{R}_{\hat{\mathbf{n}}}(\phi)) = N_\Phi \mathrm{e}^{\cos\phi}$ is a wavefunction in $SO(3)$ in the axis-angle representation $(\hat{\mathbf{n}},\, \phi)$. The orientation wavefunction

[7] The formal justification for treating a rotor like the triangle as a structureless point particle with spin, is that for integral l and $m = 0$, the rotor states, indexed by k, transform under rotations like spin states (see, e.g., [16], section 58).

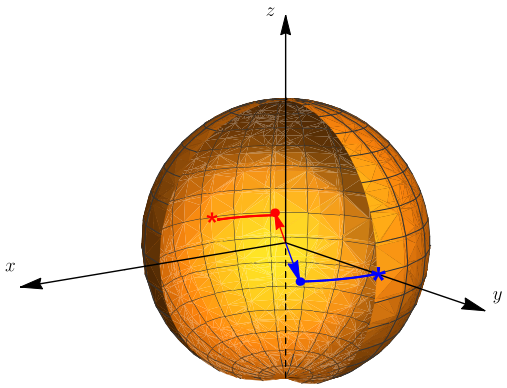

Figure 4. The stellar representation of the state $|\phi(t)\rangle$. The asteriks correspond to $t = 0$ while the dots to $t = \pi/6$.

probability density $P_\Phi = |\Phi(\phi)|^2$ has a maximum at the origin ($\phi = 0$) and decays monotonically and isotropically with increasing ϕ. $\Phi(\phi)$ itself describes a superposition of various orientations of the body frame, the amplitude for each of which depends only on the rotation angle ϕ, and is independent on the axis of rotation $\hat{n}$ between the two frames (body and space). Compared to the quantum state considered in the previous subsection, Ψ provides localization in both shape and orientation space, and is thus more appropriate for recovering the classical behavior.

We compute now the time evolution of the wavefunction (41). The Hamiltonian (35) can be separated into three, mutually commuting, terms, $H_S = (N + 1) + \omega_3(N_3 + 1/2) + \lambda^2 S^2/2$, acting on the shape variables q, $H_O = \lambda^2(\mathbf{L}^2 - L_z^2/2)$, acting on the orientation variables R, and $H_I = -\lambda^2 S L_z$, that couples q and R. The time evolution operator factorizes accordingly. To compute the action of $\mathrm{e}^{-\mathrm{i}H_O t}$ on Φ, we expand the latter in the H_O eigenfunctions $\{D^l_{km}\}$,

$$\Phi(\phi(\alpha, \beta, \gamma)) = \sum_{lkm} c^l_{km} D^l_{km}(\alpha, \beta, \gamma), \tag{46}$$

with

$$c^l_{km} = \frac{2\,l + 1}{8\pi^2} \int_0^{2\pi} \int_0^{\pi} \int_0^{2\pi} \mathrm{d}\alpha \mathrm{d}\beta \mathrm{d}\gamma \;\; \sin\beta \; D^l_{km}(\alpha, \beta, \gamma)^* \Phi(\phi(\alpha, \beta, \gamma)), \tag{47}$$

and $\phi(\alpha, \beta, \gamma) = 2\arccos(\cos\frac{\beta}{2}\cos\frac{\alpha+\gamma}{2})$. For the particular form of $\Phi(\phi)$ chosen, $c^l_{km} = c^l \delta_{km}$ holds, i.e., the expansion coefficients are non-zero only for $k = m$, and then their value only depends on l. The time-evolved orientation wavefunction then becomes

$$\Phi_t(\alpha, \beta, \gamma) = \sum_{lkm} c^l_{km} \mathrm{e}^{-\mathrm{i}\lambda^2\left(l(l+1)-k^2/2\right)t} D^l_{km}(\alpha, \beta, \gamma). \tag{48}$$

Next we easily find for $\psi_{\alpha_+,\alpha_-,t}(x_1, x_2) \equiv \mathrm{e}^{-\mathrm{i}H_S t}\psi_{\alpha_+,\alpha_-}(x_1, x_2)$,

$$\psi_{\alpha_+,\alpha_-,t}(x_1, x_2) = \mathrm{e}^{-\mathrm{i}\lambda^2 t\left(\alpha_+\tilde{\partial}_{\alpha_+} - \alpha_-\tilde{\partial}_{\alpha_-}\right)^2/2} \psi_{\alpha_+\mathrm{e}^{-\mathrm{i}t},\alpha_-\mathrm{e}^{-\mathrm{i}t}}(x_1, x_2), \tag{49}$$

since the action of the λ-independent part of H_S simply multiplies the α's by $\mathrm{e}^{-\mathrm{i}t}$, while it is easily shown that $N_\pm\,|\alpha_\pm\rangle = \alpha_\pm\tilde{\partial}_{\alpha_\pm}|\alpha_\pm\rangle \equiv \alpha_\pm(\partial_{\alpha_\pm} + \alpha^*_\pm/2)|\alpha_\pm\rangle$.

The third, coupling, term is the most interesting. Using the identity $\mathrm{e}^{\mu N_\pm} f(a_\pm) = f(\mathrm{e}^\mu a_\pm)\mathrm{e}^{\mu N_\pm}$, where f is an arbitrary analytic function, we finally find

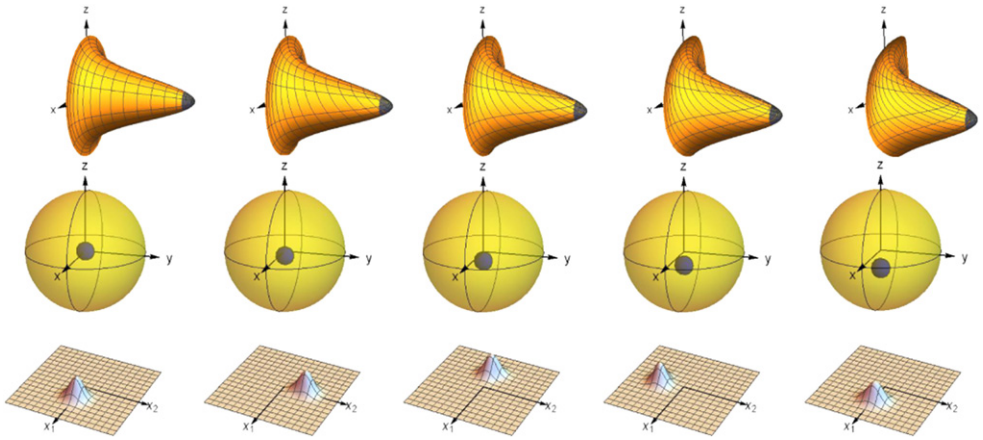

Figure 5. Sequence of the orientation change produced by a cyclic deformation in the x_1–x_2 plane in shape space for the three body problem, in the quantum case. The middle row depicts $SO(3)$, as in figure 3, while the top row contains plots of the reduced orientation probability density $P_t^O(\mathsf{R})$, restricted to the xz-plane of $SO(3)$ (elsewhere in $SO(3)$, P_t^O is obtained by rotation around the z-axis). Shown is the time evolution of the probability density associated with the initial wavefunction $\Psi(\mathsf{R}, q)$, given by (41), for $t = 2\pi n/4$, $n = 0, 1, \ldots, 4$, $\lambda = 0.2$, and $(\alpha_+, \alpha_-) = (2, 0)$. The little dark spot in the top and middle rows is the $P_t^O(\mathsf{R}) = .90 \max(P_t^O)$ surface. The plots in the bottom row are of the reduced shape probability density $P_t^S(x_1, x_2)$. While the gaussian wavefunction rotates in the $x_1 - x_2$ plane of shape space, the orientation wavefunction gets displaced along the $\hat{z}$-axis—this is the quantum analogue of the classical cat rotation.

$$\Psi_t(\alpha, \beta, \gamma, x_1, x_2, x_3) = \psi_0(x_3, t) \sum_{lkm} c^l_{km}(t) \psi^{(k)}_{\alpha_+,\alpha_-}(x_1, x_2, t) D^l_{km}(\alpha, \beta, \gamma), \tag{50}$$

where

$$\psi_0(x_3, t) = \mathrm{e}^{-\mathrm{i}\omega_3 t/2} \psi_0(x_3) \tag{51}$$

$$c^l_{km}(t) = c^l_{km} \mathrm{e}^{-\mathrm{i}\lambda^2 \left(l(l+1) - k^2/2\right) t} \tag{52}$$

$$\psi^{(k)}_{\alpha_+,\alpha_-}(x_1, x_2, t) = \mathrm{e}^{-\mathrm{i}\lambda^2 t \left(\alpha_+ \tilde{\partial}_{\alpha_+} - \alpha_- \tilde{\partial}_{\alpha_-}\right)^2/2} \psi_{\alpha_+ \mathrm{e}^{-\mathrm{i}\left(1+k\lambda^2\right)t}, \alpha_- \mathrm{e}^{-\mathrm{i}\left(1-k\lambda^2\right)t}}(x_1, x_2). \tag{53}$$

Equation (50) is valid, with the appropriate coefficients c^l_{km}, for an arbitrary initial orientation wavefunction. Taking into account the particular form of these coefficients for the $\Phi(\phi)$ we assumed above, the expression for Ψ_t simplifies to (omitting the arguments of functions)

$$\Psi_t = \psi_0 \sum_{lk} c^l \mathrm{e}^{-\mathrm{i}\lambda^2 \left(l(l+1) - k^2/2\right) t} \psi^{(k)}_{\alpha_+,\alpha_-} D^l_{kk}. \tag{54}$$

In actually computing the rhs of equation (50), or (54), one should truncate to the first order in λ^2, consistent with our expansion of the hamiltonian up to $\mathcal{O}(\lambda^2)$ (inclusive), equation (20). To be able to monitor visually the system's evolution, we start from the probability density $P_t(\mathsf{R}, q) = |\Psi_t(\mathsf{R}, q)|^2$ and compute marginal (reduced) densities

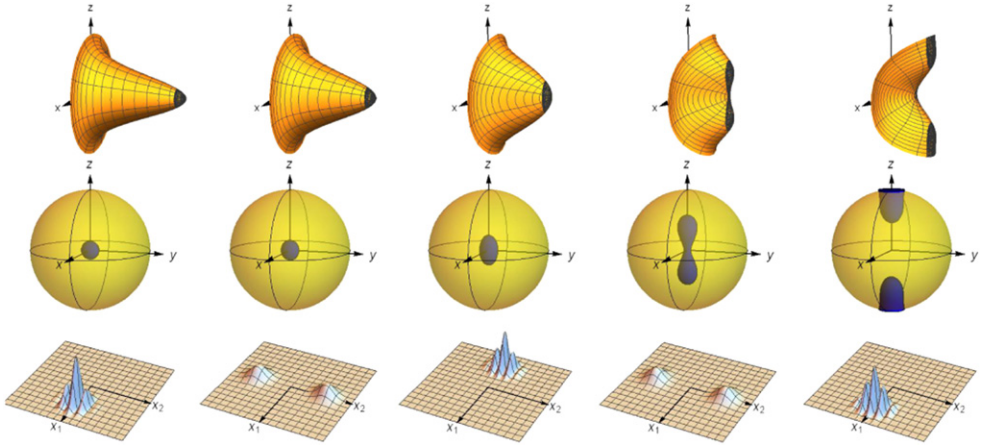

Figure 6. Evolution of the sum of the two coherent states $(\alpha_+^1, \alpha_-^1) = (3, 0)$ and $(\alpha_+^2, \alpha_-^2) = (0, 3)$. Visual conventions are as in figure 5, with $\lambda = 0.18$. The reduced shape probability in the bottom row consists of two gaussians rotating in opposite senses. This particular cyclic deformation initially elongates and eventually splits the little dark spot into two, one climbing up the $\hat{z}$-axis and the other going down (top and middle rows). This is a purely quantum scenario that can give rise to a Schroedinger cat.

$$P_t^S(q) = \int P_t(\mathsf{R}, q)\mathrm{d}\mathsf{R}, \qquad P_t^O(\mathsf{R}) = \int P_t(\mathsf{R}, q)\sqrt{g}\ \mathrm{d}^{3n-6}q, \tag{55}$$

in shape space and $SO(3)$, respectively. In figure 5 (on the previous page) we show the quantum version of the cyclic deformation and the corresponding rotation sequence, as time increases, for $(\alpha_+, \alpha_-) = (2, 0)$, which implies that $\langle S\rangle = 4$, just as in the classical situation shown in figure 3. The system rotates clockwise as its shape changes, in a fashion similar to its classical counterpart. We note as well that the surface of constant $P_t^O(\mathsf{R})$ (the little dark spot in the top and middle rows) and the width of $P_t^S(q)$ increase their size with time. Both effects are related to the dispersion of the wavefunction, the latter due to the term $\lambda^2 S^2/2$ of H_S. A quantum, quasi-rigid, triangular cat that is left to free fall with its 'feet' upwards (imagine the triangle with its plane vertical, and one of its vertices pointing upwards, marking the position of the 'feet'), should change its shape cyclically (oscillating in the x_1–x_2 plane) enough times for the little dark spot in figure 5 to reach the surface of the ball, which corresponds to a rotation (in the average sense) of π, allowing it to land safely on its feet.

3.5. Quantum righting reflex and Schroedinger cats

More exotic scenarios are of course imaginable in the quantum realm. For example, as mentioned before, if the cat oscillates in shape space in the opposite sense, then its rotation in physical space will also be in the opposite sense. Imagine then a cat that starts free falling as above, but executes a quantum superposition of the above two oscillations in shape space. In other words, its shape space wavefunction consists of two gaussians that rotate in the x_1–x_2 plane in opposite senses (figure 6, bottom row). During the fall, the cat will be in a superposition of orientation states, as it rotates both, say, clockwise and anticlockwise in physical space. As we see in the top and middle rows of figure 6, there will be two little dark spots

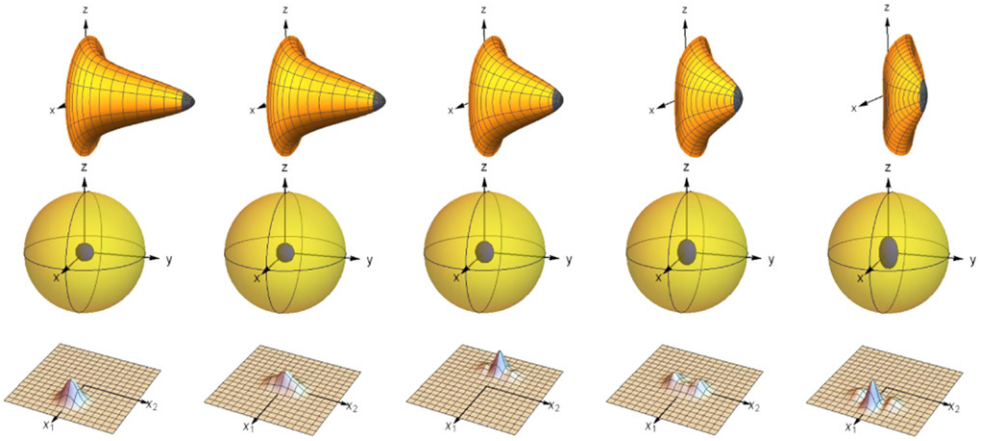

Figure 7. Conventions as in figure 5, with $\lambda = 0.35$ and $(\alpha_+, \alpha_-) = (\sqrt{2}, \sqrt{2})$, which implies $(\alpha_1, \alpha_2) = (2, 0)$. The gaussian wavefunction in this case simply oscillates along the x_1-axis, with its expectation value tracing a curve that encloses zero area. The central peak of the orientation wavefunction (dark spot at the origin of $SO(3)$) stays initially still, but gets gradually elongated along the $\hat{z}$-axis.

inside the $SO(3)$ ball, moving in opposite directions. If lucky, the cat can still land on its feet, if the two 'copies' rotate by $\pm\pi$.

Something slightly more interesting will happen if the cat does exactly as above, but is released with its feet pointing sideways (horizontally), and only has half the time available before landing. Then one copy in the quantum superposition lands on its feet, and survives the fall, while the other lands on its back, and gets killed, instantly converting the falling feline into a Schroedinger cat.

Finally, we could also fix as our initial state a wavefunction like (41), with $(\alpha_+, \alpha_-) = (\sqrt{2}, \sqrt{2})$ or, equivalently, with $(\alpha_1, \alpha_2) = (2, 0)$, which corresponds to a coherent state oscillating along x_1, with $\langle S \rangle = 0$. Also, we put $\lambda = 0.35$ to observe only the effects of dispersion. Then, comparing with the analogous classical case, the system would not be expected to rotate. Contrary to the classical case though, if left oscillating long enough, the system manages to access, with significant probability, orientations quite distinct from its initial one—see the ellipsoidal-shaped surface inside the $SO(3)$ ball in figure 7. Of course, wavefunctions tend to disperse with time, but what distinguishes this case is that the spreading out is somehow channelled along the $\hat{z}$-axis, presumably due to the oscillation in shape space—this is an aspect of the system that deserves further study. The term S^2 of the Hamiltonian tends to split the initial gaussian of $P_t^S(x_1, x_2)$ (bottom row of figure 7).

4. Implications for molecular, nuclear, and nano-systems

The effect studied in this work ought to be experimentally verifiable. Thus, e.g., a triatomic molecule, like H_3^+, set to vibrate in a state with non-zero s and vanishing angular momentum expectation value, ought to 'rotate' w.r.t. the lab (for a review about the relevance of the molecule H_3^+ in diverse physical phenomena see [21]). More accurately, its quantum state after one period of the vibration should be related to the initial one by a rotation, intermediate states being, in general, quite distinct. Our analytical results are only valid for nonlinear

molecules but, other than this limitation, do not require any particular symmetry. In fact, the presence of asymmetry may provide the means to detect the rotation. For example, if the molecule posseses permanent electric dipole moment, and a large enough population is polarized so that a macroscopic dipole moment can be measured in the lab, the excitation of suitable vibrational modes, without imparting angular momentum, should cause the dipole moment to rotate.

The scope of possible applications is actually considerably wider than triatomic molecules. The rotovibrational spectra of more complicated systems, like, for example, the ^{12}C nucleus, can be modelled surprisingly well by triangular configurations of α-particles (see, e.g., [22] for a theoretical analysis and [23], and references therein, for recent experimental results). Excited states, like the one we considered in (38), are relevant in determining spatial characteristics of the extremely important, and still largely elusive, Hoyle state (see, for example, figure 5 of [23])—effects like the one mentioned above might serve in identifying the presence of those excited states in complicated quantum superpositions. Similarly, the analysis of a four point cat model would prove relevant in tetrahedral α-particle cluster models of nuclei like ^{16}O [24].

Finally, one may envisage, in a not-so-distant future, the use of the effect studied here in the manipulation, with extreme accuracy, of the orientation of nanostructures. Suitably large molecular populations could be set to vibrate, causing an entire nanostructure containing them to reorient itself. Deexcitation of the molecules would guarantee locking an orientation while finesse could be controlled by adjustment of either the oscillation amplitude or the magnitude of the curvature tensor $\mathbf{B}$.

5. Summary and concluding remarks

Using the geometric approach to the n-body problem developed in the last decades, we presented a quantum description of the falling, reorienting, zero angular momentum cat. We recovered the classical picture assuming the cat wavefunction in shape space to be a coherent state, and also explored other, more exotic, purely quantum scenarios, including one that ends with a Schroedinger cat. Some possible applications to molecular and nuclear problems were outlined, in particular, studies of the ^{12}C nucleus, which fits nicely our triangular model due to α-particle clustering.

There is one aspect of our approach that needs to be justified. The falling cat's rotation was visualized by essentially following the maximum of the marginal probability density in $SO(3)$, rather than focusing on the 'average orientation'. The reason for this choice is that there is no 'average orientation' in a configuration space like $SO(3)$—to see this, consider the simpler case of a particle with uniform probability density around a circle, there is no meaningful assignment of an average position in this case. Thus, simply invoking Ehrenfest's theorem that the quantum description of the system will necessarily recover, through expectation values, the classical one, is not permissible here, at least not in the above naive form.

There are also some directions for further work. As mentioned already, a four-body cat would capture the non-abelian character of $SO(3)$, which is missed by our minimal, triangular model. For example, at the classical level, a four-point cat would be able to rotate around any axis, by any angle, while the three-point one studied here can only rotate around an axis perpendicular to its plane. The shape space, in the four-point case, is six dimensional, with a very complicated topological structure [7, 10]—but still, a quasi-rigid model, with its wavefunction concentrated around some equilibrium shape, should be manageable. Another

novel feature would be the appearance of degeneracy between shapes related by mirror reflection, as in the ammonia molecule, and the tunnelling between degenerate minima of the potential. Such developments would also facilitate incursions to molecular and nuclear dynamics, widening the scope of the present work —we plan on studying these matters in the near future.

Acknowledgments

The authors wish to acknowledge partial financial support from DGAPA-UNAM grant IN114712 and CONACyT grant 103486. HHC appreciates the interesting discussions with Professor B Mielnik from the Physics Department at CINVESTAV.

References

[1] Cambell L and Garnett W 2001 *The Life of James Clerk Maxwell:* With Selections from His Correspondence and Occasional Writings (Boston, MA: Adamant Media Corporation)
[2] Kane T R and Scher M P 1969 *Int. J. Solids Struct.* **5** 663–70
[3] Guichardet A 1984 *Ann. Inst. Henri Poincaré Phys. Theor.* **40** 329–42 (http://eudml.org/doc/76239)
[4] Tachibana A and Iwai T 1986 *Phys. Rev.* A **33/4** 2262–9
[5] Shapere A and Wilczek F 1989 *Am. J. Phys.* **57** 514–8
[6] Montgomery R 1993 Gauge theory of the falling cat *Dynamics and Control of Mechanical Systems* ed M J Enos (Providence, RI: AMS) pp 193218
Montgomery R 1993 Gauge theory of the falling cat *Fields Inst. Commun.* **1** 193–218
[7] Littlejohn R G and Reinsch M 1995 *Phys. Rev.* A **52** 2035–51
[8] Littlejohn R G and Reinsch M 1997 *Rev. Mod. Phys.* **69/1** 213–75
[9] Littlejohn R G, Mitchell K A, Reinsch M, Aquilanti V and Cavalli S 1998 *Phys. Rev.* A **58/5** 3705–17
[10] Littlejohn R G, Mitchell K A, Reinsch M, Aquilanti V and Cavalli S 1998 *Phys. Rev.* A **58/5** 3718–38
[11] Montgomery R 1996 *Nonlinearity* **9** 1341–60
[12] Iwai T 1992 *Phys. Lett.* A **162** 289–93
[13] Herzberg G and Longuet-Higgins H C 1963 *Discuss. Faraday Soc.* **35** 77–82
[14] Mead C A and Truhlar D G 1979 *J. Chem. Phys.* **70** 2284–96
[15] Mead C A 1992 *Rev. Mod. Phys.* **64/1** 51–85
[16] Landau L D and Lifshitz E M 1981 *Quantum Mechanics* 3rd edn (Oxford: Pergamon)
[17] Halpern M 1979 *Phys. Rev.* D **19/2** 517–30
[18] Littlejohn R and Mitchell K A 2002 Gauge theory of small vibrations in polyatomic molecules *Geometry, Mechanics, and Dynamics* ed P Newton *et al* (New York: Springer) pp 407–28
[19] Berry M V and Wilkinson M 1984 *Proc. R. Soc.* A **392** 15–43
[20] Bengtsson I and Zyczkowski K 2008 *Geometry of Quantum States* (Cambridge: Cambridge University Press)
[21] Tennyson J 1995 *Rep. Prog. Phys.* **57** 421–76
[22] Bijker R and Iachello F 2000 *Phys. Rev.* C **61** 067305
[23] Marín-Lámbarri D J, Bijker R, Freer M, Gai M, Kokalova T, Parker D J and Wheldon C 2014 *Phys. Rev. Lett.* **113** 012502
[24] Bijker R and Iachello F 2014 *Phys. Rev. Lett.* **112** 152501